

Analysis of October 23 (Mw 7.2) and November 9 (Mw 5.6), 2011 Van Earthquakes Using Long-Term GNSS Time Series

I. Tiryakioglu¹, H. Yavasoglu², M. A. Ugur¹, C. Ozkaymak³, M. Yilmaz^{1*}, H. Kocaoglu¹, B. Turgut¹

¹ Geomatics Engineering, Faculty of Engineering, Afyon Kocatepe University, TR-3200, Afyonkarahisar, Turkey.

² Department of Geomatics Engineering, Istanbul Technical University, TR-34467, Istanbul, Turkey.

³ Geology Engineering, Faculty of Engineering, Afyon Kocatepe University, TR-3200, Afyonkarahisar, Turkey.

* Correspondence: mustafayilmaz@aku.edu.tr (M.Y.).

ABSTRACT

The eastern Anatolia provides one of the best examples of an area of rapid deformation and intense contraction that is the consequence of an active continental collision between the Arabian and Eurasian plates leading to large and devastating earthquakes. The latest evidence of the active tectonism in the region is revealed by two remarkable seismic events; Van-Tabanlı (Mw 7.2, October 23, 2011) and Van-Edremit (Mw 5.6, November 9, 2011) earthquakes. The study of the earthquake cycle and observation of geodetic and seismic deformation in this region is very important to hazard assessments. In this study, the inter-seismic, co-seismic, and post-seismic movements caused by the above-mentioned earthquakes were investigated using the time series of 2300 days of Global Navigation Satellite Systems (GNSS) observations of the local stations selected from the network of the Continuously Operating Reference Stations, Turkey (CORS-TR). For the inter-seismic period, approximately 1100 daily data were obtained from 21 CORS-TR stations (prior to the earthquakes between October 1, 2008 and October 23, 2011) and evaluated using the GAMIT/GLOBK software. The behaviour of these stations was investigated by processing 1 Hz data from the GNSS stations during the earthquakes on the GAMIT/TRACK software. In addition to October 23 and November 9, the GNSS data on one day before and after the earthquakes was assessed to determine co-seismic deformations. During the October 23 earthquake, hanging-wall deformation of about 60 mm was detected in the SW direction at the MURA station. However, at the VAAN station, deformation of 200 mm (value predicted by time series) was observed in the footwall block in the NW direction. There were not any significant changes at the stations during the November 9 earthquake. For the post-seismic period, the GNSS data from 2012 to 2015 was evaluated. According to the observations, post-seismic deformation continued at the stations close to the epicenter of the earthquake.

Keywords: Van earthquake, GNSS, CORS-TR, time series

Análisis de los terremotos de octubre 23 (7.2 Mw) y noviembre 9 (5.6 Mw) de 2011 en Van a través de series temporales

GNSS a largo plazo

RESUMEN

Anatolia oriental provee uno de los mejores ejemplos de un área de rápida deformación e intensa contracción, consecuencia de una colisión continental activa entre la placa Arábiga y la Euroasiática, lo que causa grandes y devastadores terremotos. Dos notables terremotos son evidencia de la actividad tectónica de la región: los terremotos Van-Tabanlı (7.2 Mw, 23 de octubre de 2011) y Van-Edremit (5.6 Mw, 9 de noviembre de 2011). El estudio del ciclo sísmico y la observación de las deformaciones geodésicas y sísmicas en esta región es fundamental para la evaluación de riesgo. En este estudio, se investiga las fases inter-, co- y post-sísmicas asociados a estos terremotos a través de 2300 días de observaciones del Sistema Global de Navegación por Satélite (GNSS, por sus siglas en inglés) de estaciones locales seleccionadas de la red de Estaciones de Referencia de Funcionamiento Continuo en Turquía (CORS-TR). Para el periodo intersísmico se obtuvieron aproximadamente 1100 datos diarios de 21 estaciones CORS-TR (anteriores a los terremotos entre el 1 de octubre de 2008 y el 23 de octubre de 2011) y evaluados con el software GAMIT/GBLOK. El comportamiento co-sísmico fue investigado procesando datos de 1 Hz de las estaciones GNSS durante los terremotos en el software GAMIT/TRACK. Adicionalmente se evaluaron datos del GNSS un día antes y un día después de los terremotos para determinar las deformaciones cosísmicas. Durante el terremoto del 23 de octubre, en el bloque colgante se detectó una deformación de 60 mm en dirección SW (estación MURA). En la estación VAAN en el bloque yacente se observó una deformación de 200 mm en dirección NW (valor predicho por series temporales). Durante el terremoto del 9 de Noviembre no se observó cambios significativos. Para la fase post-sísmica se evaluaron los datos de la GNSS del 2012 al 2015. Según las observaciones, la deformación postsísmica continuó en las estaciones cercanas al epicentro del terremoto.

Palabras clave: Terremotos de Van; Sistema Global de Navegación por Satélite; Estaciones de Referencia de Funcionamiento Continuo en Turquía, frecuencias.

Record

Manuscript received: 21/02/2017

Accepted for publication: 28/07/2017

How to cite item

Tiryakioglu, I., Yavasoglu, H., Ugur, M.A., Ozkaymak, C., Yilmaz, M., Kocaoglu, H., & Turgut, B. (2017). Analysis of October 23 (Mw 7.2) and November 9 (Mw 5.6), 2011 Van Earthquakes Using Long-Term GNSS Time Series. *Earth Sciences Research Journal*, 21(3), 147 - 156.

Introduction

The active tectonics of Turkey are dominated by the westward tectonic escape of the Anatolian Plate, relative to Eurasia, from a collision zone between the converging African and Eurasian plates (~5 Ma) (Bozkurt 2001). The East Anatolian Contractural Province is under the control of a N-S directed compressional-contractual tectonic regime (Bozkurt 2001; Kocyigit et al. 2001; Özkaymak 2003; Özkaymak et al. 2004a, 2004b, 2011; Sengor and Kidd 1979; Sengor and Yilmaz 1981; Şaroğlu and Yılmaz 1986; Yilmaz et al. 1987). The Lake Van basin located on the north of the Bitlis-Zagros Suture Zone formed by the collision of the Eurasian and Arabian Plates suffered from historical and instrumental earthquakes of a magnitude greater than 6.0 (Ambraseys and Finkel 1995; Ergin et al. 1967; Soysal et al. 1981). The most recent of these were the Mw=7.2 Tabanlı-Van earthquake of October 23, 2011 and the Mw=5.6 Edremit earthquake of November 9, 2011 (Figure 1) (USGS 2011). According to the field-based geologic and seismic geomorphology studies performed soon after the earthquake (Akyuz et al. 2011; Emre et al. 2011; Özkaymak et al. 2011), the Mw 7.2 earthquake occurred on an ENE-striking and north-dipping 70-km-long main thrust fault which was named the Van Fault Zone (VFZ) by Emre et al. (2011). The northern block (hanging-wall) of the thrust fault moved towards the southern block. The reported depth of the hypocenter is about 16 km and the co-seismic thrust offset was approximately 2 m around the hypocenter (Akyuz et al. 2011; KOERI 2011; USGS 2011). According to studies using Synthetic Aperture Radar interferometry after the earthquake, the hanging-wall uplift was about 80 cm (Akyuz et al. 2011). The focal mechanism solution of the November 9, 2011 earthquake and the results of geological studies in the region indicate that the Mw 5.6 earthquake occurred on the NE-SW-trending Edremit Fault (EF) with a sinistral strike-slip character.

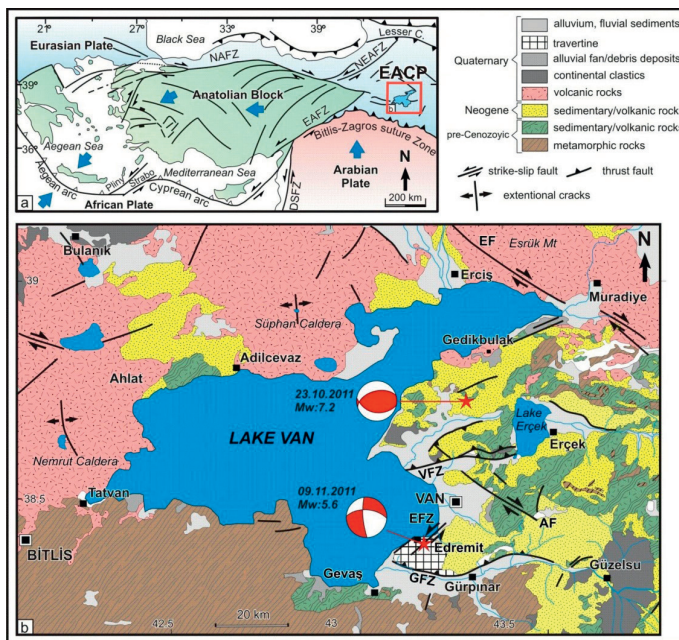


Figure 1. (a) Tectonic outline of the eastern Mediterranean area.

Abbreviations: EACP, East Anatolian Contractural Province; DSFZ, Dead Sea Fault Zone; EAFZ, East Anatolian Fault Zone; NAFZ, North Anatolian Fault Zone; (b) Lake Van Basin and simplified geological map showing the main tectonic structures of the Lake Van Basin and the surrounding area.

Abbreviations: GFZ: Gürpınar Fault Zone, AF: Alabayir Fault, VFZ: Van Fault Zone, EFZ: Edremit Fault Zone, EF: Ercis Fault (compiled from Emre et al. (2012); Özkaymak et al. (2004a), (2011); Şenel (2002)).

The results of other social and geodetic studies in relation to the tectonics of the region can be found in the relevant references (McClusky et al. 2000; Ozener et al. 2010; Reilinger et al. 2006; Tatar et al. 2012; Yavasoglu et al. 2011; Zare and Nazmazar 2013). Studies carried out

after the October 23, 2011 earthquake investigated the amount of dislocation caused by the earthquake using the data from the CORS-TR stations in the region. However, these studies only focused on co-seismic deformation (Altiner et al. 2013; Yildirim et al. 2014). Dogan et al. (2014) determined the post-seismic deformation using the data obtained from the GNSS network after the earthquake. However, research in this area is still limited, thus there is a need for further studies to investigate post-seismic deformation to provide a better and complete understanding of the earthquake cycle of the region.

In this study, the inter-seismic, co-seismic, and post-seismic movements of the two earthquakes were investigated simultaneously with the GNSS time series of the local reference stations selected from the CORS-TR Network. For the inter-seismic period, approximately 1100 daily data were obtained from 21 CORS-TR stations (during the pre-earthquake period from October 1, 2008 to October 23, 2011) and evaluated using the GAMIT/GLOBK software. The behaviour of these stations was investigated by processing 1 Hz data from the GNSS stations during the earthquakes on the GAMIT/TRACK software. In addition to October 23 and November 9, the GNSS data in one day before and after the earthquakes was assessed to determine co-seismic deformations. For the post-seismic period, the GNSS data from 2012 to 2015 was evaluated and time series were obtained. Findings from the time series analysis showed that there were local movements in some of the CORS-TR stations (MALZ, MUUS, SIRN and HAKK). These movements indicate that the post-seismic deformation continued around the stations located close to the earthquake epicenter.

The Tectonic Structure of the Region

The Lake Van Basin is located just north of the Bitlis-Zagros Thrust Zone that was formed by the collision of the Arabian and Eurasian plates (Figure 1). It is also situated to the east of the Karlova Triple conjunctions at the intersection of the North Anatolian Fault and East Anatolian Fault. Since the collision to date, the region has been uplifted approximately 2 km (Kocyigit et al. 2001). The active tectonic structures observed in the region include NW-SE-trending right lateral (e.g., Ercis, Cildiran, and Alabayir faults), NE-SW-trending left-lateral strike-slip faults (eg. Edremit Fault Zone), approximately E-W-trending reverse/thrust faults (e.g., Van Fault Zone and Gürpınar Fault Zone), and NS-trending extensional faults associated with volcanic activity (e.g., Nemrut opening and Suphan opening). These structures indicate approximately N-S-directed compressional-contractual tectonic regime in the region (Figure 1) (Emre et al. 2012; Özkaymak et al. 2004a; 2011; Şenel, 2002). The Van Fault Zone (VFZ) consists of a large number of E-W-trending north-dipping parallel/semi-parallel thrust fault splays. The first of these was identified by Özkaymak (2003) in the Holocene lacustrine/fluvial sediments striking 70° N and dipping 45° NW with a dominant thrust and minor left-lateral character. According to the surface deformations of the October 23, 2011 earthquake and geomorphologic observations, VFZ is mapped approximately 30 km along the zone between Lake Van to the west and south of the Lake Erçek to the east (Emre et al. 2011) (Figure 1). Another E-W-trending and north-dipping major neotectonic structure in the Lake Van Basin is the Gürpınar Fault Zone (GFZ) located in the southeast of Lake Van (Figure 1). Özkaymak et al. (2004a) suggested that this thrust fault could also be the source of the 2003 earthquake (Mw 4.7) in Edremit. According to the focal mechanism solution of the 2003 earthquake and the geological mapping studies in the region, as a result of this event, the Quaternary travertine deposits were thrust over the younger fluvial deposits towards the south. The fault generating the November 9, 2011 earthquake (Mw 5.6) was mapped by Özkaymak (2003) and called the Edremit Fault. The NE-SW-trending left-lateral strike-slip Edremit fault cuts and deforms the Quaternary Edremit travertines and can be traced to a distance of approximately 10 km. The Alabayir Fault located in the east of Van is a NW-SE-trending right-

lateral strike-slip fault of approximately 32 km (Özkaymak 2003). Datasets of historical and instrumental earthquakes indicate that many destructive earthquakes and surface ruptures occurred along these active structures reflecting the geodynamic setting of the Lake Van Basin and the surrounding area. Several events with the intensity of 9 and higher have been reported for the historical period, including 1110, 1441, 1647, 1696, and 1881 (Ambraseys and Finkel 1995; Ergin et al. 1967; Soysal et al. 1981). However, the source faults of these events are still not clear. During the instrumental period, the focal mechanism solutions of some moderate-scale earthquakes that occurred between 1988 and 2002, the most recent earthquake on October 23, 2011 (Mw 7.2), and a large number of aftershocks demonstrate that E-W-trending thrust faults are active. Furthermore, NE-SW- and NW-SE-trending strike-slip faults are also observed in the region.

GNSS network and data analysis

CORS-TR is a nationwide GNSS network established in Turkey through a project implemented by Istanbul Kultur University (IKU) in collaboration with the General Command of Mapping and General Directorate of Land Registry and Cadastre between 2006 and 2009 and sponsored by the Scientific and Technological Research Council of Turkey (TUBITAK) (Eren et al. 2009). One of the objectives of this project was to establish a spatial infrastructure to monitor the tectonic plate movements using continuous GNSS data, ultimately to contribute to the prediction of earthquakes and early warning studies within the network area (Uzel et al. 2013).

The CORS-TR network has 21 reference stations located near the epicentres of the Van earthquakes, covering a total area of ~ 100000 km² (Figure 2). The closest station to the epicentres of both Van earthquakes is VAAN at a distance of 21 km and the furthest is ARDH at a distance of approximately 275 km.

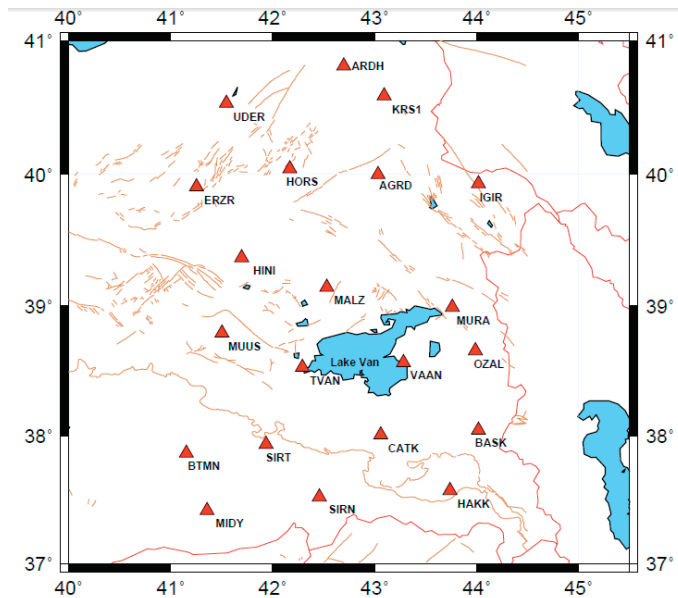


Figure 2. The CORS-TR stations evaluated in the study

In this study, 2300 days of GNSS observations of the 21 CORS-TR stations were recorded at 30-second intervals in the RINEX data format (01.10.2008-31.12.2014, covering inter-seismic, co-seismic and post-seismic periods). The data from the GNSS day 2008.75 to 2015.00 was processed on a daily basis on the GAMIT/GLOBK software (Herring et al. 2010).

Data from each daily measurement were processed using two International Terrestrial Reference Frames (ITRF); ITRF2008 and ITRF08_EURA. As in many studies, the following processing parameters are used in this research. The antenna phase center was derived according to the

height-dependent model. The precise orbit information (IGS-F) in the SP3 format required by the GAMIT process was downloaded from the Scripps Orbit and Permanent Array Center (SOPAC) database (Herring et al. 2010). The Earth rotation parameters (ERPs) were obtained from United States Naval Observatory Bulletin B (USNO Bull. B). LC (L3) the ionosphere-independent linear combination of the L1 and L2 carrier waves was used during the analysis. The FES2004 Ocean Tide Loading (OTL) grid was used to interpolate the components of the displacement caused by ocean tides (Gulal et al. 2013; Herring et al. 2010; Lyard et al. 2006; Ozener et al. 2010; Tiryakioglu et al. 2013; Tiryakioglu 2015).

Analysis of inter-seismic deformation with long-term time series and inter-seismic strain field

For the inter-seismic period, time series of station coordinates (ITRF08 and ITRF08_EURA) were obtained from the GAMIT software starting with the first measurement taken at the time of the earthquake (2008.75-2011.85). With the time series analysis, it is possible to determine the linear (trend), periodic and irregular (stochastic) movements of the reference stations. For the north, east, and up coordinates of the reference stations, the time series of $x(t_i)$ depending on the time of t_i ($i=1,2,3,\dots,N$) can be expressed as follows (Gulal et al. 2013, 2015):

$$\bar{x}(t_i) = \underbrace{\sum_{k=1}^m a_k t_i^{k-1}}_{\text{trend component}} + \underbrace{\sum_{s=1}^r [b_s \cos(2\pi f_s t_i) + c_s \sin(2\pi f_s t_i)]}_{\text{periodic component}} + \underbrace{\sum_{j=1}^p \alpha_j \bar{x}(t_{i-j})}_{\text{Stochastic component}} + \underbrace{\sum_{jj=1}^q \beta_{jj} v(t_{i-j})}_{\text{Stochastic component}} + \underbrace{v(t_i)}_{\text{Random Errors}} \quad (1)$$

where,

a_k : Trend component parameters,

b_s ; c_s : Periodic component parameters,

f_s : Frequency,

α_j : Auto-regressive (AR (p)) model parameters,

β_{jj} : Average Movement (MA (q)) model parameters,

$v(t_i)$: Random errors with average zero and variance σ^2

$m, k; r, s; p, j; q, jj$: Degree and order of the time series.

In order to perform the time series analysis of $x(t_i)$, the data must be continuous and systematic. In the analysis of the time series, first, the general state of time series should be visually interpreted based on the time-dependent graphics of the series. In the time series of the 21 reference stations located in the study area, some measurements were observed to have sudden and non-recurring peaks. These measurements called 'outliers' provide values that are either significantly smaller or larger than the average values of the time series. In this study, we discuss the 'additive outliers' (AO), first defined by Fox (1972) as the first type outliers that occur due to incorrect data entry or measurements, and affect only one measurement. After the removal of the measurements that are significantly larger or smaller than the expected values, the time series returns to its normal course (Gulal et al. 2013).

In cases where some of the measurements of the $x(t_i)$ series are affected by AO at time t_i , the new series that is obtained can be expressed by $y(t_i)$ as in the following Eq. (2).

$$y(t_i) = AO(t_i) + \bar{x}(t_i) \quad (2)$$

Outliers in time series are usually determined using a function that fits the series. The function used to eliminate outliers in the $y(t_i)$ series can be expressed as the sum of linear and trigonometric functions (periodic motion) (Erdogan 2012; Gulal et al. 2013).

The analysis of the trend component in the coordinate time series derived from the GNSS data is crucial for earth sciences since the linear movements of time series, ' $a_k \cdot t$ ' in the trend component are used to determine the plate movements (or velocity) based on the time unit and the direction (Gulal et al. 2013; Gulal et al. 2015). It is also assumed that annual periodic

movements are produced by the effect of atmospheric and hydrologic loading (Blewitt and Lavallee 2002; Wdowski et al. 1997). Furthermore, Van Dam et al. (2001) and Romagnoli et al. (2003) suggested that due to the climatic effects such as the accumulation of ice on antennas and antenna shields, there are periodic movements that occur quarter-yearly, half-yearly and yearly.

The outliers in the time series of $y(t)$ were detected using the method described by Gulal et al. (2015) and then these outliers were removed from the series. To avoid complexity, the stochastic component was not added to the function. The same function can be used to estimate new values for missing data due to the removal of outliers. Furthermore, as shown in Figures 3A and 4A, this function can estimate values to fill the gaps caused by GNSS data loss.

To determine the temporal movements of the GNSS stations, the coefficients of the linear function that fits the time series were estimated using the software developed in MATLAB (Figure 3B-4B). The inter-seismic velocities of the stations were determined by the estimated coefficients (Figure 5) using the core stations of the International GNSS Service (IGS).

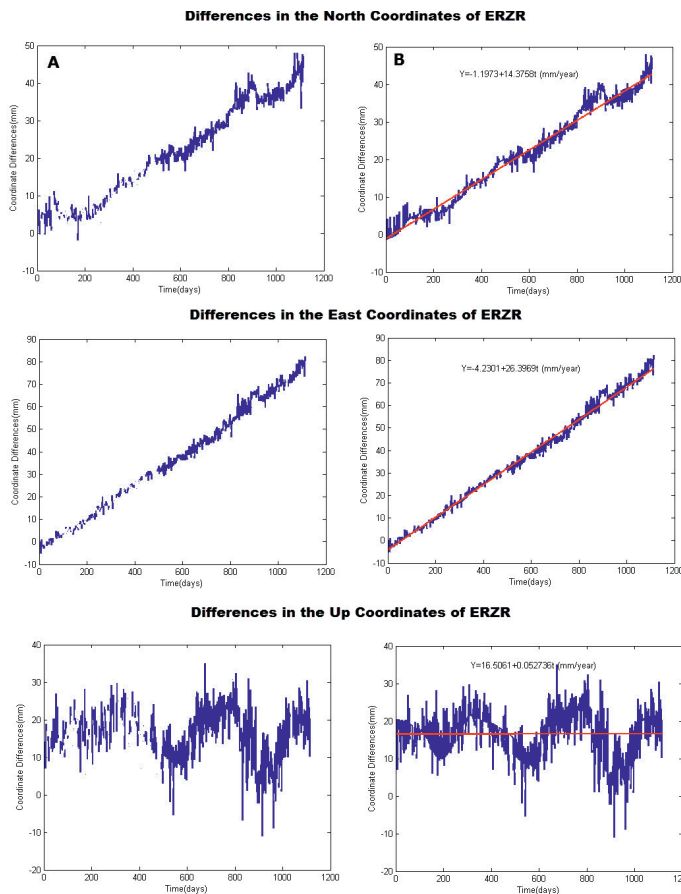


Figure 3. Time series (Column A) and linear function (Column B) for the components in the north, east, and up coordinates of the ERZR station in ITRF08

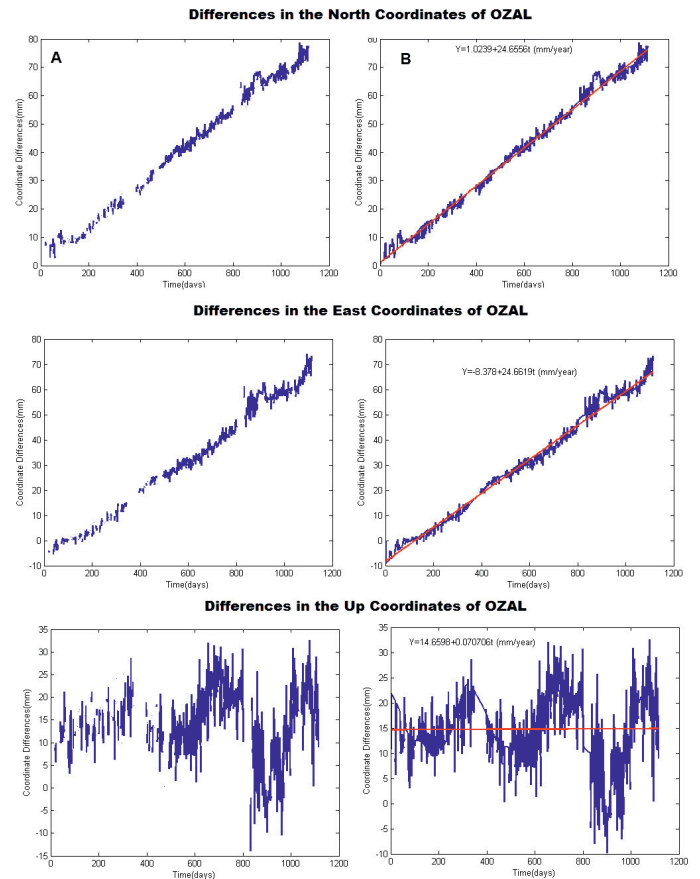


Figure 4. Time series (Column A) and linear function (Column B) for the components in the north, east, and up coordinates of the OZAL station in ITRF08

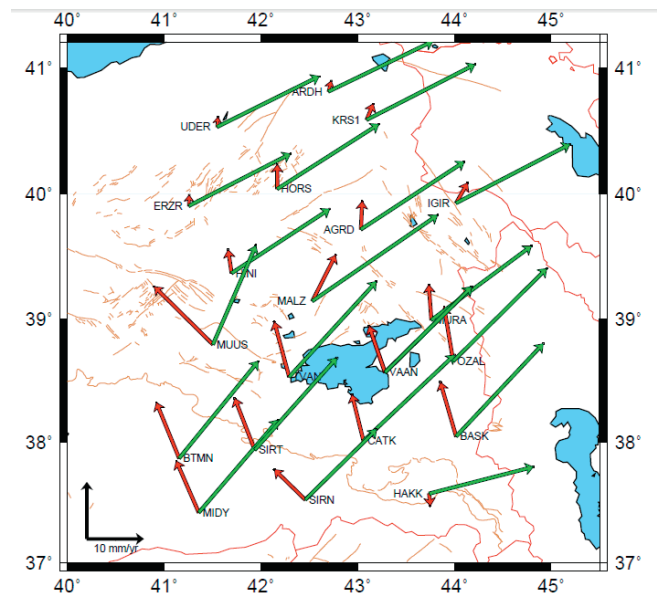


Figure 5. Velocities obtained from the time series analyses; the red arrows indicate Eurasia-fixed velocities and the green arrows shows ITRF08 velocities.

Based on Figure 5, it was observed that the MALZ, MUUS, SIRM, and HAKK stations move in different directions compared to other stations due to local movements (Ozdemir 2016). Furthermore, some sudden fluctuations were identified at the MALZ and MUUS stations

(Figure 6). The Normalized Root Mean Square (NRMS) values of these stations are ± 4.1 mm, ± 5.8 mm, ± 3.1 mm; ± 6.0 mm, ± 4.6 mm, ± 1.3 mm, respectively. Furthermore, for these stations, the annual, semi-annual, and seasonal periodic movements explained earlier were found to be greater. This can be attributed to the changes in water level according to seasons and varied amount of precipitation. Although no fluctuations were observed in the time series of the HAKK and SIRN stations, they acted in a way contrary to the region's tectonic structure. This might be due to local deformations that occurred at these stations.

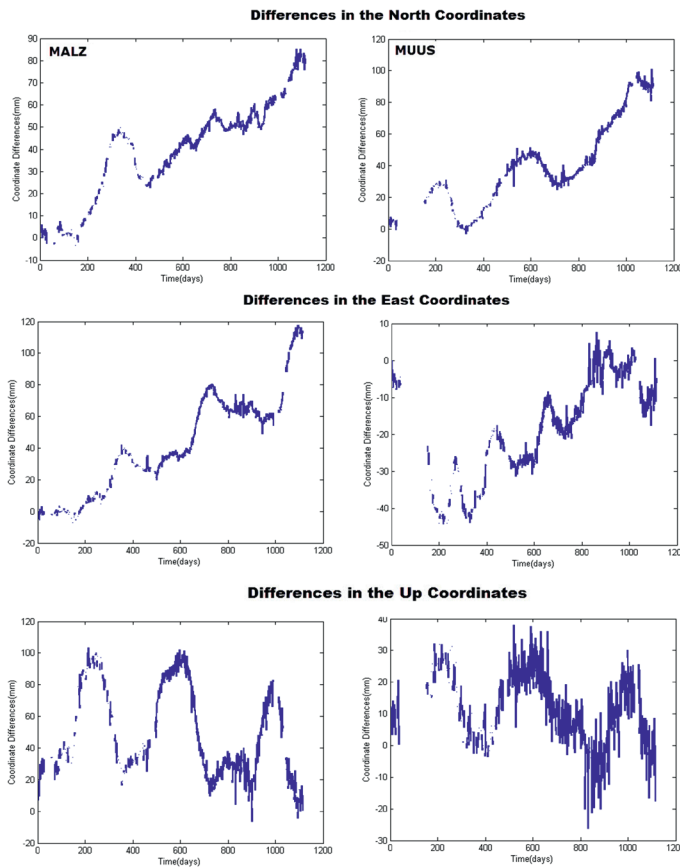


Figure 6. Time series of the components in the north, east, and up coordinates of the MALZ and MUUS stations in ITRF08.

Calculation of the Inter-seismic Strain Rate

The strain analysis was performed using the inter-seismic velocities to obtain the strain fields of the region. For reasons explained in detail earlier in the paper, the MALZ, MUUS, HAKK, and SIRN stations were excluded from the analysis. After determining the velocity vectors, the stress and strain parameters of the region were calculated. In the literature, various methods have been suggested for the determination of stress and strain parameters (Brunner 1979; Deniz 1990; Dogan 2002; Kakkuri and Chen 1992; Lambeck 1988).

In this study, the GNSS sites were used to create geodetic triangles, and from these triangles, the strain rates were calculated. The general approach associated with this method is to obtain a strain field of the east and north velocity components determined through the analysis of time series. Figure 7 presents the calculated strain rates of the generated triangles. The MIDY station was excluded from figure 7 because of the geometric distortion.

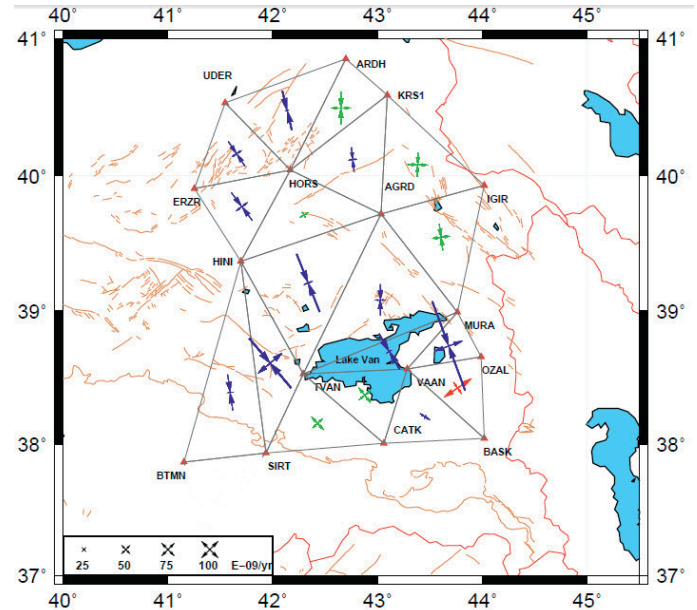


Figure 7. Geodetic triangles and the strain rates

In Figure 7, the dominant extension areas, pure compression areas and the strike-slip faults are indicated by red, blue and green arrows, respectively.

Figure 7 shows that compressions consistent with the tectonic regime are widely seen. The largest compressions in the region were observed in the NNW-SSE direction, located in the triangles of MURA-OZAL-VAAN (-128 E-09/yr), HINI-TVAN-SIRT (-88 E-09/yr) and HINI-AGRD-TVAN (-84 E-09/yr). The October 21 earthquake occurred in the MURA-OZAL-VAAN triangle. This demonstrates, once again, that the focal mechanism solution of the earthquake complies with the strain. The United States Geological Survey (USGS) observed a rotation of 66 degrees in the NNE direction from the earthquake solutions and 50-70 degrees from the surface measurements (USGS 2011). In the strain analysis, the rotation of the axis direction was found to be 70 degrees in the NNE direction. The largest extension was observed in the ENE-WSW direction and located in the VAAN-OZAL-BASK (46 E-09/yr) triangle. Furthermore, strike-slip faults were observed in the south of Lake Van in the TVAN-VAAN-CATK and TAVN-CATK-SIRT triangles. The EFZ fault is another example of these strike-slip faults. The focal mechanism solutions of the November 9 earthquake in EFZ in the TVAN-VAAN-CATK triangle comply with the strain. In addition, in the AGRD-IGIR-MURA triangle, strike-slips are active in the north of Lake Van. The Caldiran fault located in the same region is another strike-slip fault that is in compliance with the 1976 earthquake (Ms:7.3) solutions (Tan et al. 2008). Similarly, the solutions of the November 15, 2000 earthquake (Mw: 5.6) in the same triangle indicate the presence of strike-slip faults in the region (Pinar et al. 2007).

Determination of Co-seismic Motion and Deformation

In order to determine the co-seismic motion, 1 Hz GNSS data obtained from the CORS-TR stations in the region were analyzed (10:00 to 11:00 UTC on Oct. 23, 2011, doy296). Since the 1 Hz GNSS data of the November 9 earthquake was not available, this earthquake was excluded from this study. Furthermore, some of the CORS-TR stations in the region were not operational on October 23, 2011; therefore, the co-seismic motions of these stations were not analyzed due to the lack of data. As a result, the co-seismic motions of 11 stations were analyzed (MALZ, IGIR, HAKK, MURA, OZAL, TVAN, SEMD, SIRT, MUUS, HINI, and HORS).

The kinematic positions of the 11 stations were determined using the kinematic data processing program, TRACK developed at Massachusetts Institute of Technology. TRACK version 1.21, released with the GAMIT/GLOBK version 10.4 (Herring et al. 2010) and the IGS final orbits were used to determine the kinematic baseline lengths. The displacement components of the 11 stations were plotted as differences in one-second-epoch coordinates relative to the reference coordinates of the stations. Figure 8 presents the co-seismic motions of the MALZ, HAKK, and MURA stations between 10:40:00 and 10:45:00 UTC. Similar results were observed in the TVAN, SEMD, OZAL, IGIR stations. There were no significant changes in the SIRT, MUUS, HINI, and HORS stations.

The coordinates of the stations obtained in the days before and after the earthquakes were evaluated to determine the co-seismic deformations of both earthquakes. As mentioned earlier, outliers were detected and removed from the series. New values were estimated using a linear function that fit the series. From the GNSS data one day before and after the earthquake was not available for all stations; the missing coordinates in the series were estimated using the linear functions. The post-seismic earthquake data for the VAAN station was derived using a logarithmic function as explained in Section 3.4.

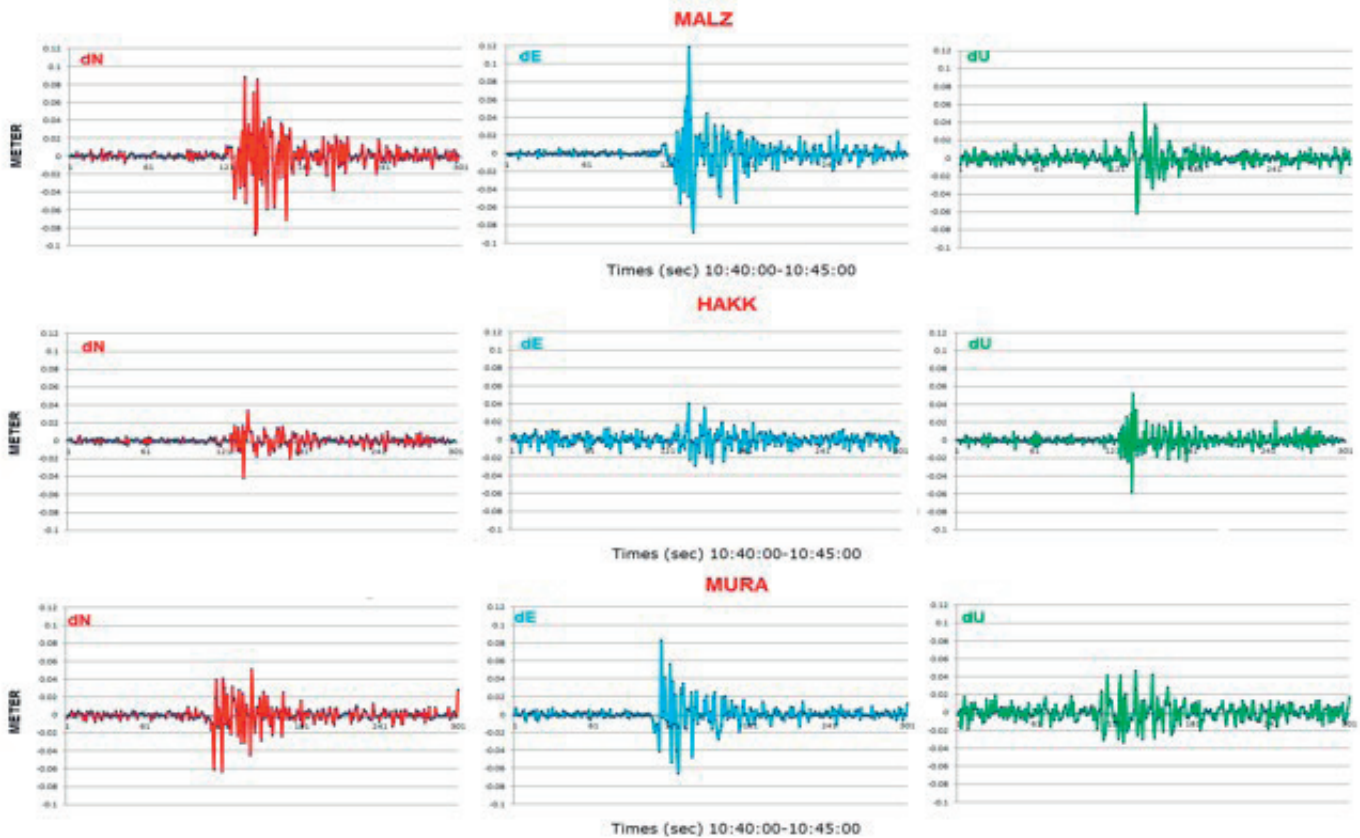


Figure 8. Velocity waveforms at the MALZ, HAKK, and MURA stations during the earthquake along the three coordinates

The inter-seismic 1 Hz kinematic solution of MURA (the closest station to the earthquake epicenter, Van-Ercis) shows the maximum movements as 11.5 ± 1.5 cm in the direction of N-S, 14.8 ± 1.3 cm in the direction of E-W, and 6.9 ± 3.2 cm in the vertical direction. Similarly, the maximum movements of the OZAL station were 14.2 ± 1.5 cm in the direction of N-S, 7.6 ± 1.6 cm in the direction of E-W, and 7.0 ± 3.6 cm in the vertical direction. The highest displacement was obtained from the MALZ station with the movement being 17.5 ± 1.5 cm in the direction of N-S, 20.5 ± 1.6 cm in the direction of E-W and

12.1 ± 3.2 cm in the vertical direction. Contrary to Altiner et al. (2013), in the current study, the MALZ station was observed to have shaken more, despite being further from the earthquake epicenter compared to the MURA and OZAL stations.

The analysis of co-seismic deformation showed that the November 9, 2011 earthquake did not cause any deformation in the trends of the GNSS stations, whereas the October 23, 2011 earthquake caused deformation to the GNSS stations, as mentioned in Konca 2015. (Figure 9)

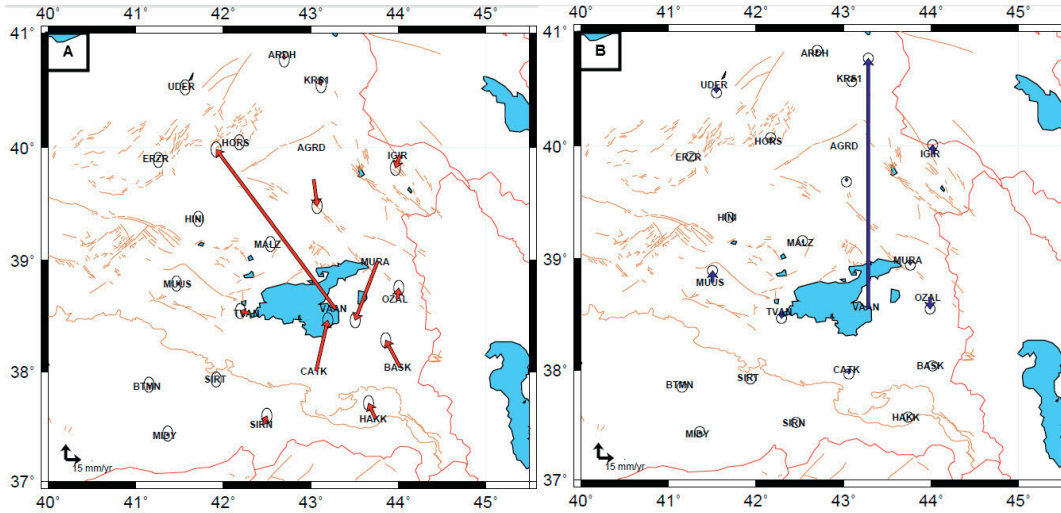


Figure 9. Co-seismic deformations. The red arrows indicate horizontal movements (A) and the blue arrows show vertical movements (B).

Figure 9 shows that the largest co-seismic deformation occurred at the VAAN station with a movement of 226 ± 3 mm in the direction of NW. This supports the data reported by other studies (Altiner et al. 2013; Dogan et al. 2014). In addition, at this point, a positive movement (169 ± 5 mm) was found in the vertical direction. This shows that the VAAN station is on the footwall block (Figure 9B).

In the stations to the north of the earthquake epicenter (on the hanging block), deformations were in the S-SW direction, whereas in the stations to the south of the earthquake epicenter (on the footwall block) deformations were in the direction of N-NW. This indicates that deformations are compatible with the characteristics of the respective earthquake. Despite the high number of interseismic movements in the MALZ station (Figure 8), there was almost no co-seismic deformation. Furthermore, no co-seismic deformation was observed in the BTMN, MIDY, SIRT, and MUUS stations.

Post-seismic Deformation

In order to determine the post-seismic deformation, 1100-days of data from post-earthquake years (between 2012.0 and 2015.0) was processed using the GAMIT software. The coordinates of the stations relative to the Eurasian plate were analyzed using time series as described in Section 3.1. According to the time series analysis, the post-seismic deformation of the VAAN station did not show any linear trends.

The linear function is not suitable for the analysis of time series data obtained after a megathrust earthquake. The time series of the VAAN station can be characterized with a logarithmic relaxation function (Figure 10). Satirapod et al. (2008) found that a Logarithmic decay function presented by Marone et al. (1991) better fits the post-seismic time series of the 2011 earthquakes.

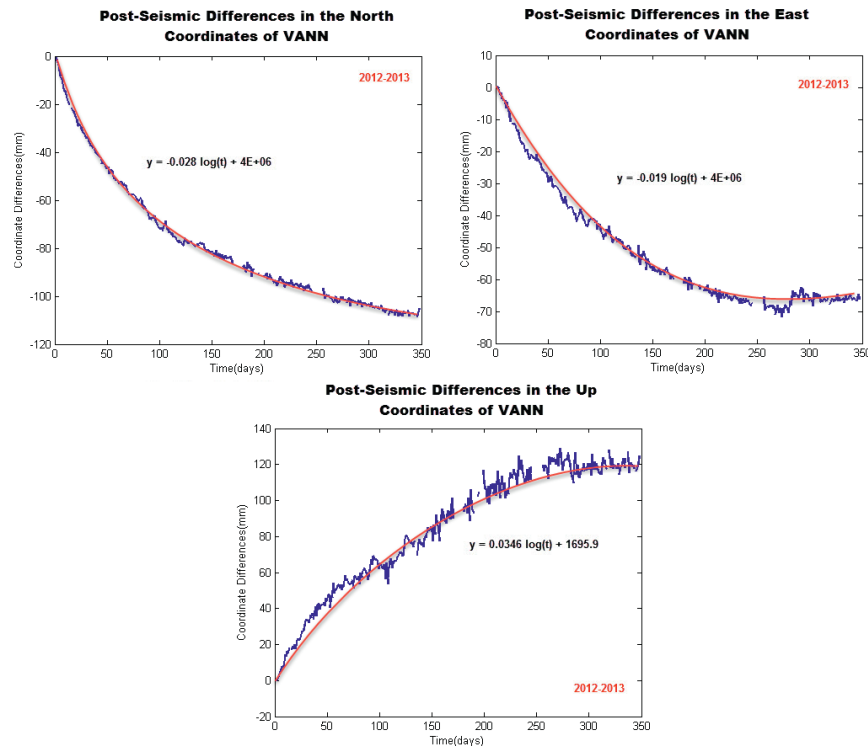


Figure 10. Time series of the VAAN station. The thin curved line in red fits the changes in coordinates as a logarithmic function of $a + b \log(t)$ (where t is time after the earthquake in years, and a and b are constants) (Savage et al. 2005).

The functions of time series are used to derive velocity combinations with respect to different years to determine whether the post-seismic movements continue (Figure 11). The accuracy of all velocity combinations was found to be lower than ± 1 mm/year. The black arrows in Figure 11 indicate the pre-seismic velocities presented in Figure 5. At the VAAN station, which is the nearest station to the epicenter of the earthquake, the post-seismic velocity between 2012 and 2013 is 131 ± 1 mm in the direction of EW which is significantly different from the pre-seismic velocity. Furthermore, the MURA and AGRD stations which are also close to the earthquake epicenter move in the SE direction contrary to the pre-seismic velocity. However, in the BASK, CATK, TVAN, OZAL, and HINI stations the pre-seismic and post-seismic directions are similar with the only difference being an increase in the post-seismic velocities. The post-seismic and inter-seismic velocities are almost the same in other stations further from the epicenter of the earthquakes; such as the SIRN, MIDY, BTMN, and SIRT stations.

After the earthquake, the VAAN station has been re-constructed 10 km away from its initial location and was renamed as VAN1. This new location is on the same hanging block as the VAAN station. The post-

seismic velocity of VAN1 for the years between 2012 and 2014 is 26 mm greater than the pre-seismic velocity of the VAAN station. However, both velocities are in the NW direction. The MURA and AGRD stations changed their direction of motion from SE to E. Contrary to the previous year, their post-seismic velocities decreased getting closer to their inter-seismic velocities.

Despite the 6mm decrease in the post-seismic velocity of the VAN1 station from 2012 to 2015, it was still 20 mm greater than the pre-seismic velocity. The TVAN and MURA stations were renamed as TVA1 and MUR1 following their movement after the earthquake. For all stations except the VAN1, OZAL, BASK, CATK, MURA, and AGRD stations, the post-seismic and pre-seismic velocities were almost the same. However, the stations closer to the earthquake epicenter such as VAN1, BASK, and CATK still had post-seismic movements.

The analysis of the post-seismic velocities of the GNSS stations between 2013 and 2015 demonstrated that the post-seismic motion was transformed into an inter-seismic motion.

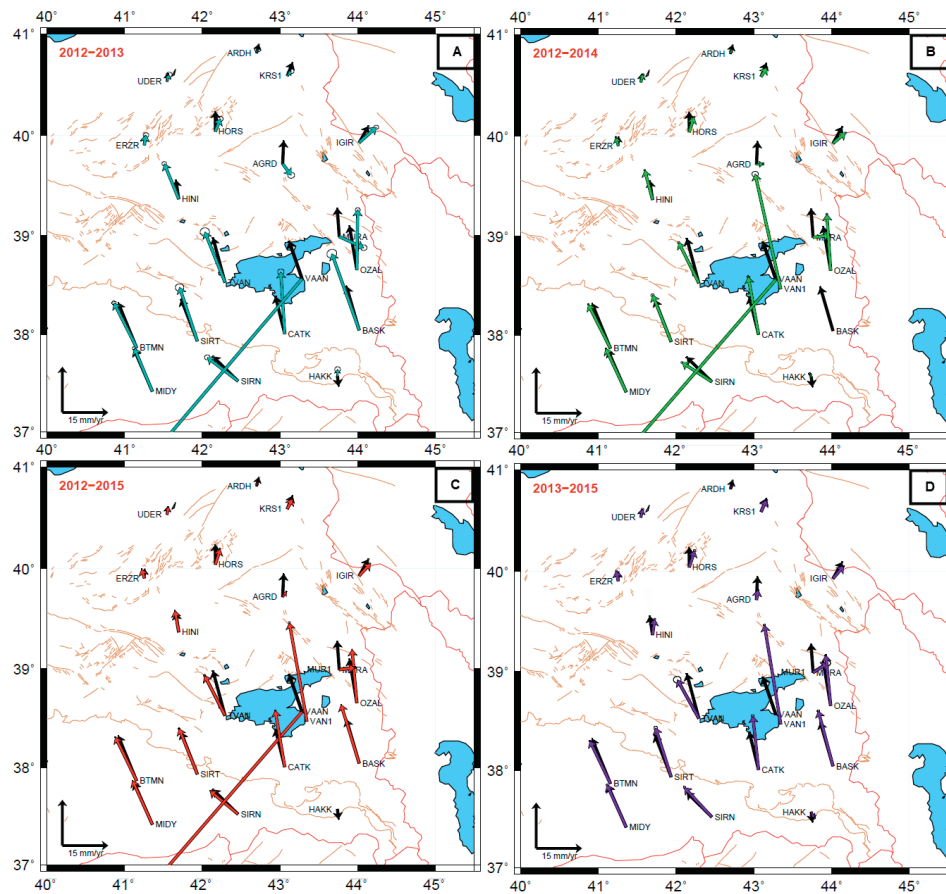


Figure 11. Post-seismic motions by periods. The red, green, purple and turquoise arrows indicate horizontal movements.

Conclusions

In this paper, a total of 2300 daily data was obtained from the GNSS observations of 21 CORS-TR stations (between 2008.75 and 2015.00) using the GAMIT software. The coordinates of the stations were determined on a daily basis according to ITRF08 and ITRF08_EURA. The outliers were eliminated from the time series. The trends of these time series were used to derive the velocities of the GNSS stations.

The period from October 1, 2008 to October 23, 2011 was evaluated in terms of the inter-seismic movements. Based on the analysis of the inter-seismic time series at the MALZ and MUUS stations, the annual periodic differences were considered to have been caused by changes

in ground water level. It was also observed that there were some local deformations at the HAKK and SIRN stations. Therefore, these four stations were not included in the strain analysis. The largest compressions in the region were observed in the VAAN-MURA-OZAL triangle, which indicates that the thrust faults are active. The focal mechanism solutions of the October 23, 2011 earthquake showed that the earthquake occurred on a thrust fault. The directions of the compressions were found to be in agreement with the solutions of the earthquake. Furthermore, the focal mechanism solutions of the 2011 earthquakes and the previous earthquakes that had occurred in the region were consistent with the results of the strain fields. This also indicates the possibility that the thrust faults are active particularly in the south of Lake

Van. Strain analysis is a powerful method to predict the possible strong ground motions in a region. As in the case of HINI-AGRD-SIRT region (figure 7), strain values indicate the approximately NNW-SSE directional compressional tectonic regime. It means that the thrust faults located at the west of VFZ can produce destructive earthquakes in the future.

The co-seismic displacements were determined only for 11 stations due to the lack of 1 Hz GNSS data for the co-seismic period for the remaining stations. Despite not being the closest station to the earthquake epicenter, the MALZ station was affected most (Figure 8). Earthquakes may cause different movements at the roof level depending on the dynamic character of the buildings. For a building with a lower horizontal rigidity, the motion of the roof is greater than the ground motion. The ground facility type of the MALZ station is a pillar. Therefore, it is considered that MALZ had been affected most since its GNSS receivers on the building measured not only the ground motion, but also the motion of the building relative to the ground motion.

The VAAN station had a logarithmic trend after the earthquake, which continued for approximately a year. After re-construction to new location (VAN1), its trend became linear.

According to the analysis of inter-seismic deformation calculated from the stations on the footwall block, the direction is NNW while the stations on the hanging block, the direction is SSW. The VAAN station was located close to the deformation zone, 400 meters away from the surface rupture caused by the earthquake. Therefore, it was observed that the VAAN station was uplifted about 17 cm due to the thrust fault movement.

In terms of the post-seismic deformation, after slip was normally the main physical mechanism for the ground motion after the main shock. We processed the continuous GNSS data to create deformation maps and calculate the variations in time-series. Furthermore, the results indicate the potential presence of a low angle fault splay as suggested by Dogan et al. (2014).

We also processed the post-seismic data in four periods, 2012-2013, 2012-2014, 2012-2015 and 2013-2015 (Figure 11). The post-seismic movement was composed of thrust slip with a significant left-lateral component in the region affected by the main shock. Both left-lateral and thrust components of the post-seismic slip are in agreement with the results of earlier studies (Dogan et al. 2014; Feng et al. 2014). The post-seismic deformation was found to have different rotational components when the velocities were determined from the time for different periods (Figure 11). The IGIR, MURA and AGRD stations, in particular, underwent unequal rotational deformation throughout the four periods. After the earthquake, the stress may have been shifted to the northern and western part of the region.

Acknowledgment

This study was supported by Afyon Kocatepe University's project numbered 13.FEN.BIL.038. We thank the university staff for their invaluable support and recommendations throughout the study.

References

- Akyüz, S., Zabcı C. & Sançar, T. (2011). Preliminary report on the 23 October 2011 Van earthquake. Faculty of Mines, Istanbul Technical University, Istanbul.
- Altiner, Y., Söhne, W., Güney, C., Perlt, J., Wang R. & Muzli M. (2013). A geodetic study of the 23 October 2011 Van, Turkey earthquake. *Tectonophysics*, 588, 118-134. DOI:10.1016/j.tecto.2012.12.005
- Ambraseys, N.N. & Finkel, C.F. (1995). *The seismicity of Turkey and adjacent areas: A historical review, 1500-1800*. Istanbul: M.S. Eren, Eren Yayıncılık.
- Blewitt, G. & Lavallee, D. (2002). Effect of annual signals on geodetic velocity. *Journal of Geophysical Research-Solid Earth*, 107 (B7), ETG 9-1-ETG 9-11. doi:10.1029/2001jb000570
- Bozkurt, E. (2001). Neotectonics of Turkey – a synthesis. *Geodinamica Acta*, 14 (1-3), 3-30. doi:10.1016/S0985-3111(01)01066-X
- Brunner, F.K. (1979). On the analysis of geodetic networks for the determination of the incremental strain tensor. *Survey Review*, 25 (192), 56-67. doi:10.1179/sre.1979.25.192.56
- Deniz, R. (1990). Jeodezik ölçmelerden yerkabuğundaki lokal gerilimlerin belirlenmesi. (in Turkish) *Journal of Istanbul Technical University*, 48, 15-22.
- Doğan, U. (2002). 17 Ağustos 1999 İzmit Depreminden Kaynaklanan Deformasyonların Kinematik Modellerle Araştırılması. Dissertation in Turkish, Yıldız Technical University.
- Doğan, U., Demir, D. Ö., Çakır, Z., Ergintav, S., Ozener, H., Akoğu, A.M., . . . , Reilinger, R. (2014). Postseismic deformation following the Mw 7.2, 23 October 2011 Van earthquake (Turkey): Evidence for aseismic fault reactivation. *Geophysical Research Letters*, 41 (7), 2334-2341. doi:10.1002/2014gl059291
- Emre, Ö., Duman, T., Özalp, S. & Elmacı, H. (2011). 23 Ekim 2011 Van depremi saha gözlemleri ve kaynak faya ilişkin ön değerlendirmeler. (in Turkish) vol 22. *General Directorate of Mineral Research & Exploration (MTA)*, Ankara
- Emre, Ö., Duman, T., Olgun, Ş., Elmacı, H. & Özalp, S. (2012). 1/250000 ölçekli Türkiye Diri Fay Haritası Serisi. (in Turkish). *General Directorate of Mineral Research & Exploration (MTA)*, Ankara
- Erdogan, H. (2012). The effects of additive outliers on time series components and robust estimation: A case study on the Oymapinar Dam, Turkey. *Experimental techniques*, 36 (3), 39-52. doi:10.1111/j.1747-1567.2010.00676.x
- Eren, K., Uzel, T., Gulal, E., Yildirim, O. & Cingoz, A. (2009). Results from a Comprehensive Global Navigation Satellite System Test in the CORS-TR Network: Case Study. *Journal of Surveying Engineering-Asce*, 135 (1), 10-18. doi:10.1061/(asce)0733-9453(2009)135:1(10)
- Ergin, K., Guclu, U. & Uz, Z. (1967). Türkiye ve civarının Deprem Katalogu (MS 11-1964). vol 24. Maden Fakültesi Arz Fizigi Enstitüsü yayımları (in Turkish), Istanbul Technical University
- Feng, W., Li, Z., Hoey, T., Zhang, Y., Wang, R., Samsonov, S., . . . , Xu, Z. (2014). Patterns and mechanisms of coseismic and postseismic slips of the 2011 M-w 7.1 Van (Turkey) earthquake revealed by multi-platform synthetic aperture radar interferometry. *Tectonophysics*, 632, 188-198. doi:10.1016/j.tecto.2014.06.011
- Fox, A.J. (1972). Outliers in time series. *Journal of the Royal Statistical Society Series B (Methodological)*, 34 (3), 350-363.
- Gülal, E., Erdoğan, H. & Tiryakioğlu, I. (2013). Research on the stability analysis of GNSS reference stations network by time series analysis. *Digital Signal Processing*, 23 (8), 1945-1957. doi:10.1016/j.dsp.2013.06.014
- Gülal, E., Dindar, A.A., Akpınar, B., Tiryakioğlu, I., Aykut, N.O. & Erdoğan, H. (2015). Analysis and management of GNSS reference station data. *Tehnicki Vjesnik-Technical Gazette*, 22 (2), 407-414. Doi: 10.17559/TV-20140717125413
- Herring, T.A., King, R.W., Floyd, M.A. & McClusky, S.C. (2010). Introduction to Gamit/Globk, Release 10.4 Report. Department of Earth, Atmospheric, and Planetary Sciences, Massachusetts Institute of Technology, Cambridge
- Kakkuri, J. & Chen, R.H. (1992). On horizontal crustal strain in Finland. *Bulletin Geodesique*, 66 (1),12-20. doi:10.1007/bf00806806
- Kocycigit, A., Yilmaz, A., Adamia, S. & Kuloshvili, S. (2001). Neotectonics of East Anatolian Plateau (Turkey) and Lesser Caucasus: Implication for transition from thrusting to strike-slip faulting. *Geodinamica Acta*, 14 (1), 177-195. doi:10.1016/s0985-3111(00)01064-0
- KOERI (2011). 23 October 2011 Van Earthquake (Mw 7.2) Evaluation Report. *Kandilli Observatory and Earthquake Research Institute (KOERI)*, Istanbul
- Konca, A. O. (2015). Rupture process of 2011 Mw7.1 Van, Eastern Turkey earthquake from joint inversion of strong-motion, high-rate GPS, teleseismic, and GPS data, *J. Seismol.*, 19 (4), 969-988, doi:10.1007/s10950-015-9506-z.
- Lambeck, K. (1988). *Geophysical geodesy-The slow deformations of the earth. vol 1*. Oxford University Press, Oxford: Clarendon.

- Lyard, F., Lefevre, F., Letellier, T. & Francis, O. (2006). Modelling the global ocean tides: Modern insights from FES2004. *Ocean Dynamics*, 56 (5-6), 394-415. doi:10.1007/s10236-006-0086-x
- Marone, C.J., Scholtz, C.H. & Bilham R (1991). On the mechanics of earthquake afterslip. *Journal of Geophysical Research-Solid Earth and Planets*, 96 (B5), 8441-8452. doi:10.1029/91jb00275
- McClusky, S., Balassanian, S., Barka, A., Demir, C., Ergintav, S., Georgiev, I., . . . Veis, G. (2000) Global Positioning System constraints on plate kinematics and dynamics in the eastern Mediterranean and Caucasus. *Journal of Geophysical Research-Solid Earth*, 105 (B3), 5695-5719. doi:10.1029/1999jb900351
- Ozdemir, S. (2016) TUSAGA ve TUSAGA-Aktif istasyonlarının hassas koordinat ve hızlarının hesaplanması üzerine (in Turkish). *Journal of Mapping*, 155, 53-81.
- Ozener, H., Arpat, E., Ergintav, S., Dogru, A., Cakmak, R., Turgut, B. & Doğan, U. (2010) Kinematics of the eastern part of the North Anatolian Fault Zone. *Journal of Geodynamics*, 49 (3), 141-150. doi:10.1016/j.jog.2010.01.003
- Özkaymak, Ç. (2003) *Van şehri ve yakın çevresinin aktif tektonik özellikleri (Active Tectonic Properties of Van City and Nearby Area)*. Master Thesis in Turkish, Yüzüncü Yıl University
- Özkaymak, Ç., Yürür, T. & Köse, O. (2004a). *An example of intercontinental active collisional tectonics in the Eastern Mediterranean region (Van, Eastern Turkey)*. Paper presented at the Fifth International Symposium on Eastern Mediterranean Geology (5th ISEMG), Thessaloniki, Greece.
- Özkaymak, Ç., Sağlam, A. & Köse, O. (2004b). *Van Gölü doğusu aktif tektonik özellikleri*. Paper presented at the 7th Annual ATAG (Active Tectonics Research Group) Meeting, Yüzüncü Yıl University, Van (in Turkish),
- Özkaymak, Ç., Sözbilir, H., Bozkurt, E., Dirik, K., Topal, T., Alan, H. & Çağlan, D. (2011). 23 Ekim 2011 Tabanlı-Van Depreminin Sismik Jeomorfolojisi ve Doğu Anadolu'daki Aktif Tektonik Yapılarla Olan İlişkisi (Seismic Geomorphology of October 23, 2011 Tabanlı-Van Earthquake and Its Relation to Active Tectonics of East Anatolia). *Journal of Geological Engineering*, 35 (2), 175-200. (in Turkish)
- Pinar, A., Honkura, Y., Kuge, K., Matsushima, M., Sezgin, N., Yilmazer, M. & Ögütçü, Z. (2007). Source mechanism of the 2000 November 15 Lake Van earthquake (M-w=5.6) in eastern Turkey and its seismotectonic implications. *Geophysical Journal International*, 170 (2), 749-763 doi:10.1111/j.1365-246X.2007.03445.x
- Reilinger, R., McClusky, S., Vernant, P., Lawrence, S., Ergintav, S., Cakmak, R., . . . , Karam, G. (2006). GPS constraints on continental deformation in the Africa-Arabia-Eurasia continental collision zone and implications for the dynamics of plate interactions. *Journal of Geophysical Research-Solid Earth*, 111 (B5) doi:10.1029/2005jb004051
- Romagnoli, C., Zerbini, S., Lago, L., Richter, B., Simon, D., Domenichini, F., . . . , Ghirotti, M. (2003). Influence of soil consolidation and thermal expansion effects on height and gravity variations. *Journal of Geodynamics*, 35 (4), 521-539. doi:10.1016/s0264-3707(03)00012-7
- Satirapod, C., Simons, W.J.F. & Promthong, C. (2008). Monitoring deformation of Thai geodetic network due to the 2004 Sumatra-Andaman and 2005 Nias earthquakes by GPS. *Journal of Surveying Engineering-Asce* 134 (3), 83-88. Doi:10.1061/(asce)0733-9453(2008)134:3(83)
- Savage, J.C., Svarc, J.L. & Yu, S.B. (2005). Postseismic relaxation and transient creep. *Journal of Geophysical Research-Solid Earth*, 110 (B11) doi:10.1029/2005jb003687
- Sengor, A.M.C. & Kidd, W.S.F. (1979). Post-collisional tectonics of the Turkish-Iranian plateau and a comparison with Tibet. *Tectonophysics*, 55 (3), 361-376. Doi:10.1016/0040-1951(79)90184-7
- Sengor, A.M.C. & Yılmaz, Y. (1981). Tethyan evolution of Turkey - a plate tectonic approach. *Tectonophysics*, 75 (3-4), 181-241 doi:10.1016/0040-1951(81)90275-4
- Soysal, H., Sipahioğlu, S., Kolçak, D. & Altınok, Y. (1981). Türkiye ve Çevresinin Tarihsel Deprem Kataloğu, MÖ. 2100-MS. 1900 (Historical Earthquake Catalogue of Turkey and Its Surroundings, BC. 2100-AD. 1900). TUBİTAK - *Scientific and Technical Research Council of Turkey*, Project Report No. TBAG-341 (in Turkish)
- Şaroğlu, F. & Yılmaz, Y. (1986). Doğu Anadolu'da neotektonik dönemdeki jeolojik evrim ve havza modelleri MTA Dergisi. *Bulletin of the Mineral Research and Exploration*, 107, 61-83. (in Turkish)
- Şenel, M. (2002). Türkiye Jeoloji Haritası (Geological map of Turkey, scale 1: 500,000, 19 sheets). . *General Directorate of Mineral Research & Exploration (MTA)*, Ankara.
- Tan, O., Tapırdamaz, M.C. & Yörük, A. (2008) The earthquake catalogues for Turkey. *Turkish Journal of Earth Sciences*, 17, 405-418.
- Tatar, O., Poyraz, F., Gürsoy, Ö., Çakır, Z., Ergintav, S., Akpınar, Z., Yavaşoğlu (2012). Crustal deformation and kinematics of the Eastern Part of the North Anatolian Fault Zone (Turkey) from GPS measurements. *Tectonophysics*, 518-521, 55-62. doi:10.1016/j.tecto.2011.11.010
- Tiryakioğlu, I., Floyd, M., Erdoğan, S., Güllal, E., Ergintav, S., McClusky, S. & Reilinger, R. (2013). GPS constraints on active deformation in the Isparta Angle region of SW Turkey. *Geophysical Journal International*, 195 (3), 1455-1463. doi:10.1093/gji/ggt323
- Tiryakioğlu, I. (2015). Geodetic aspects of the 19 May 2011 Simav earthquake in Turkey. *Geomatics Natural Hazards & Risk*, 6 (1), 76-89. doi:10.1080/19475705.2013.831379
- USGS (2011) Magnitude 7.1 - EASTERN TURKEY. *The United States Geological Survey (USGS)* retrieved from <https://earthquake.usgs.gov/earthquakes/eventpage/usp000j9rr#executive>. Accessed 25 December 2015
- Uzel, T., Eren, K., Güllal, E., Tiryakioğlu, I., Dindar, A.A. & Yılmaz, H. (2013). Monitoring the tectonic plate movements in Turkey based on the national continuous GNSS network. *Arabian Journal of Geosciences* 6 (9), 3573-3580. doi:10.1007/s12517-012-0631-5
- Van Dam, T., Wahr, J., Milly, P.C.D., Shmakin, A.B., Blewitt, G., Lavallee, D. & Larson, K.M. (2001). Crustal displacements due to continental water loading. *Geophysical Research Letters* 28 (4), 651-654. doi:10.1029/2000gl012120
- Wdowinski, S., Bock, Y., Zhang, J., Fang, P. & Genrich, J. (1997). Southern California permanent GPS geodetic array: Spatial filtering of daily positions for estimating coseismic and postseismic displacements induced by the 1992 Landers earthquake. *Journal of Geophysical Research-Solid Earth* 102 (B8), 18057-18070. Doi:10.1029/97jb01378
- Yavasoglu, H., Tari, E., Tuysuz, O., Cakir, Z. & Ergintav, S. (2011). Determining and modeling tectonic movements along the central part of the North Anatolian Fault (Turkey) using geodetic measurements. *Journal of Geodynamics* 51 (5), 339-343. doi:10.1016/j.jog.2010.07.003
- Yildirim, O., Yaprak, S. & Inal, C. (2014) Determination of 2011 Van/Turkey earthquake (M = 7.2) effects from measurements of CORS-TR network. *Geomatics Natural Hazards & Risk* 5: (2), 132-144. doi:10.1080/19475705.2013.789453
- Yılmaz, Y., Saroglu, F. & Guner, Y. (1987) Initiation of the neomagmatism in East Anatolia. *Tectonophysics* 134, 177-199. doi:10.1016/0040-1951(87)90256-3
- Zaré, M. & Nazmazar, B. (2013) Van, Turkey Earthquake of 23 October 2011, Mw 7.2; An overview on disaster management. *Iranian Journal of Public Health*, 42(2), 134-144.